Validation of Computational Simulation for Tumor-treating Fields with Homogeneous Phantom

Ma, M, Fu, G, Wang, M, Liu, H, Zheng, D, Pan, Y & Zhang, S

Validation of Computational Simulation for Tumor-treating Fields with Homogeneous Phantom

Mingwei Ma, Guihang Fu, Minmin Wang, Haipeng Liu, Dingchang Zheng, Yun Pan and Shaomin Zhang*

Abstract— **Tumor-treating Fields (TTFields) is a promising cancer therapy technique in clinical application. Computational simulation of TTFields has been used to predict the electric field (EF) distribution in the human body and to optimize the treatment parameters. However, there are only a few studies to validate the accuracy of the simulation model. Here we propose a measurement platform with technical details for validating the simulation model of TTFields. We further constructed homogeneous agar phantoms with different conductivity for voltage measurement. With the measured voltages from six equidistance recording points in the cylinder phantom, we calculated the EF intensity in the phantoms at different frequencies. Comparing the measured values with the simulated values obtained from two types of source simulation, we found that the current source simulation model of TTFields is a reliable method for evaluating the EF intensity distribution.**

I. INTRODUCTION

Tumor-treating Fields (TTFields) is a non-invasive cancer therapy technique, which delivers specific frequency (100 to 300 kHz) and low intensity (1 to 3 V/cm) alternating electric fields to disrupt the cell division and inhibit the proliferation of tumor cells [1, 2]. Several studies have demonstrated that the inhibitory effect of TTFields was influenced by many factors, such as stimulation intensity, frequency, and dosage [1-3].

The spatial electric fields (EF) induced by TTFields within a specific biological tissue are one of the most significant contributing factors to its clinical effects. However, it is difficult to obtain the EF distribution by in *vivo* measurement.

As an alternative way, the computational models of TTFields have been developed to understand the spatial EF distributions within the human body [4, 5]. Many types of computational models were proposed from spherical head models to realistic head models based on individual structural magnetic resonance imaging (MRI) data which includes scalp, skull, cerebrospinal fluid (CSF), gray matter (GM), or other tissues [4, 5]. It is a good visual and practical tool to predict the spatial EF distribution during TTFields. With individual modeling, the stimulation parameters can be optimized to improve the effects in a specific target region theoretically. However, despite sophisticated simulation models have been applied, there is still a lack of in *vivo* evidence to assess and validate the prediction performance of the simulation model. Kirson *et al.* reported one case of measuring the TTFields intensity within the human brain, but no specific in *vivo* results were disclosed [2]. Blatt *et al.* compared the simulated voltages with the practical measured values in rats without analyzing the tissue property [6]. The computational models have not been validated enough. It is a remarkable fact that the actual spatial EF distribution in the human body remains largely unclear during different TTFields conditions. The insufficiency of understanding limits principled efforts to mechanism research and stimulation optimization.

In recent years, we also observed that several studies proposed in *vitro* measurement methods for validating the tES (transcranial electrical stimulation) simulation model [7, 8]. Compared with in *vivo* validation, it has higher operability and repeatability. Wang *et al.* proposed to mimic the conductivity of human brain tissue by mixing the agar powder with a suitable NaCl solution, and building a multi-layer head model assembly with different conductivity agar phantom, they found that there was a high correlation between theoretical value and measured voltage when tDCS was applied [7]. Taken together, although agar phantom cannot perfectly imitate human tissue, it is an operational and repeatable method to validate the simulation model of TTFields.

Here, we aim to validate the accuracy of simulation models by directly measuring EF distribution with agar phantom in *vitro*. In addition, we further study the impact of stimulation frequency, transducer contact medium, and tissue type on induced EF of TTFields.

II. MATERIALS AND METHODS

A. Measurement platform

To measure the EF distribution of TTFields, we constructed an experimental platform. As shown in Fig.1C, the experiment platform consists of a digital stereotaxic frame (68028, RWD, Shenzhen, China), a waveform generator (DG2502, RIGOL, Beijing, China), two probes, and a phantom module.

Fig.1B shows the phantom module including the transducers, conductive gel, copper plates, and the agar phantom. We prepared two agar phantoms with different

Mingwei Ma, Minmin Wang, and Shaomin Zhang* are with Qiushi Academy for Advanced Studies, Provincial Key Laboratory of Cardio-Cerebral Vascular Detection Technology and Medicinal Effectiveness Appraisal Zhejiang University, Hangzhou, 310027, China (e-mail: {mamina, wangmin217, shaomin}@zju.edu.cn).

Guihang Fu and Yun Pan are with the College of Information Science and Electronic Engineering, Zhejiang University, Hangzhou 310027, China (e-mail: {22060278, panyun}@zju.edu.cn).

Haipeng Liu and Dingchang Zheng are with the Research Centre of Intelligent Healthcare, Coventry University, Coventry, United Kingdom (e-mail: {ad4828, dingchang.zheng}@coventry.ac.uk).

conductivity: agar_σ0.78 and agar_σ0.48, which represent the conductivity of 0.78 S/m and 0.48 S/m, and their radius and length are 17 mm and 50 mm respectively. The reason why we chose the conductivity of 0.48 S/m was that the conductivity of the muscle tissue is close to 0.48 S/m at 500 kHz frequency [9], and we wanted to validate the EF distribution in muscle tissue *in vitro* in the future. To study the influence of the contact medium between the transducer and agar phantom, we prepared two different conductive gels: gel_σ0.75 and gel_σ4.5, which represent the conductivity of 0.75 S/m and 4.5 S/m.
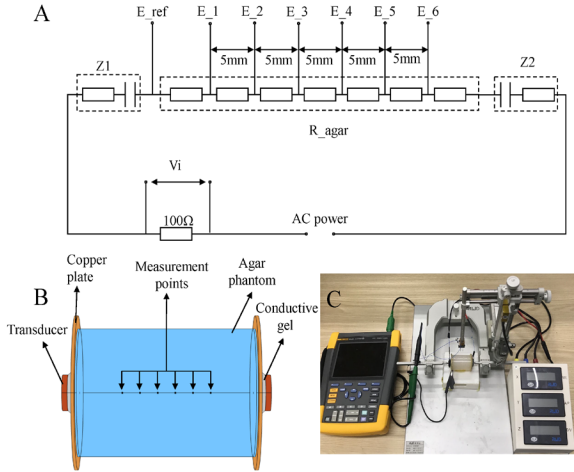

Figure 1. A. The equivalent circuit model of the measurement process. B. The structure of the agar phantom module. C. Picture of the measurement platform.

Fig.1A shows the equivalent circuit model of the measurement process:

- AC power generates 20 V, 50 to 500 kHz sinusoidal signals.

- A 100 Ω sample resistor in series is used to calculate the current.

- Z1 and Z2 represent the contact impedance between the agar phantom and wires, including equivalent capacitance and resistance.

- R_agar means the whole resistance of the agar phantom.

- E_ref is the reference point, which connects the reference terminal of the scopemeter, and E_1, E_2, E_3, E_4, E_5, and E_6 are the six measuring points in the agar phantom, connecting the other terminal of the scopemeter.

Fig.1B shows the location of the six recording points, which are on the central axis of the agar phantom in equidistant distribution of 5 mm.

Firstly, the two probes were fixed on the stereotaxic frame, and the spacing and depth of the two probes were set to 5 mm and 17 mm respectively. Then adjusted the axes of the stereotaxic frame to move the probes to the measuring points in the agar phantom. After measuring the voltages of Vi (shown in Fig.1C) and the probes, adjusted the stereotaxic frame to the next two measuring points until all of the points

were measured. During the whole measuring process, the voltage of the power supply remained unchanged and the frequency ranged from 50 to 500 kHz.

We got three different datasets in total: Dataset1 (D1), Dataset2 (D2), and Dataset3 (D3). D1 was the dataset using agar_σ0.78 and gel_σ4.5. D2 was the dataset using agar_σ0.78 and gel_σ0.75. D3 was the dataset using agar_σ0.48 and gel_σ4.5. We were able to validate the simulated data of different conductivity agar phantoms by comparing D1 and D3 and explore the influence of contact medium by comparing D1 and D2.

B. Phantom construction

We can assign the conductivities of the phantom using agar/ NaCl mixtures. Ionic mobility of added salts is a major factor influencing the conductivity in solution [10]. As a result, the conductivity of the agar phantom increases with the increase of NaCl concentration. We mixed the powdered agar with proper NaCl and de-ionized water to mimic the conductivity of various tissues. Firstly, the NaCl solution was heated to about 65 °C. Secondly, Powdered agar was dissolved in hot NaCl solution and stirred with a magnetic stir bar, continuously heating to about 95 °C, and then air-cooled for 4 min. Finally, the agar solution was poured into corresponding 3D printed cylindrical molds. After the agar solution was cooled down, the mold was removed to release the agar phantoms as shown in Fig.1C.

C. Simulation model

Since the stimulation wavelength of TTFields is significantly larger than the phantom size, the EF phase variation is negligible across this region. Maxwell's equation in a quasi-static approximation is suitable for this TTFields model [11]. The electrical field distribution for the model is governed by the Laplace equation [12]:

$$\nabla \cdot (\sigma \nabla V) = 0$$

V is the electric potential and σ is the conductivity. The whole agar phantom module was modeled (Shown in Fig.1B) and the permittivity and conductivity were assigned.

Most TTFields modeling studies set the constant current source as a stimulation condition[5, 13-15], and only a few simulation models selected the constant voltage source [16]. To compare the differences in simulated EF between the two stimulation conditions, and further validate the accuracy of the simulation model, we modeled the two stimulation conditions respectively. Additionally, because the current and voltage across the agar phantom varies with the stimulation frequency in practical measurement, we set the measured current and voltage at each frequency as the simulation parameters in modeling. The finite element method (FEM) was used to calculate the spatial distribution of induced electric potential.

D. Data acquisition and analysis

The voltages were measured by a floating scopemeter (Fluke-190-II-series, FLUKE, Romania), and the current in the circuit was calculated by the 100 Ω sample resistor in each dataset. Electric field intensities of the agar phantom were

calculated through every two measured points' voltages dividing the distance of probes. According to Ohm's Law, we got the actual impedance of the non-agar phantom module, which included the contact impedance at different frequencies. Percentage variation was used to evaluate the differences between the simulated values and measured values.
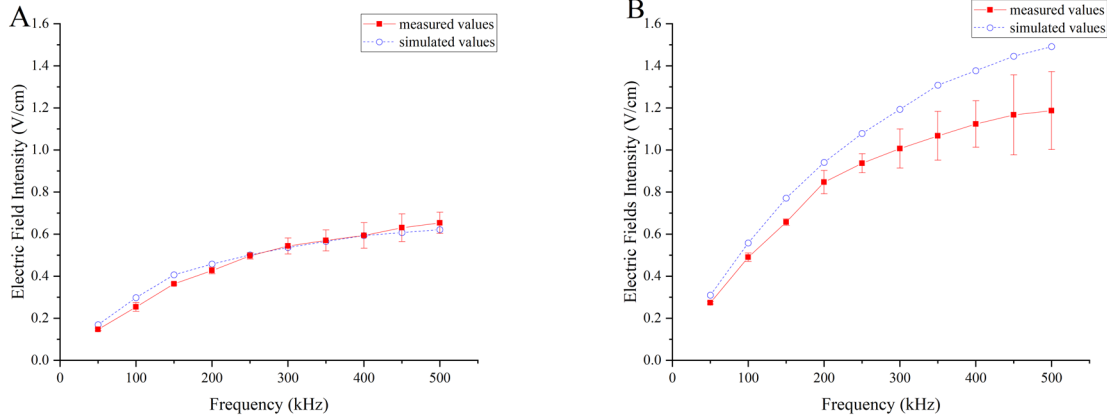

Figure 2. A. Measured and simulated electric field intensity of agar_σ0.78 phantom at different frequencies under the constant current source simulation condition. B. Measured and simulated electric field intensity of agar_σ0.48 phantom at different frequencies under the constant current source simulation condition.
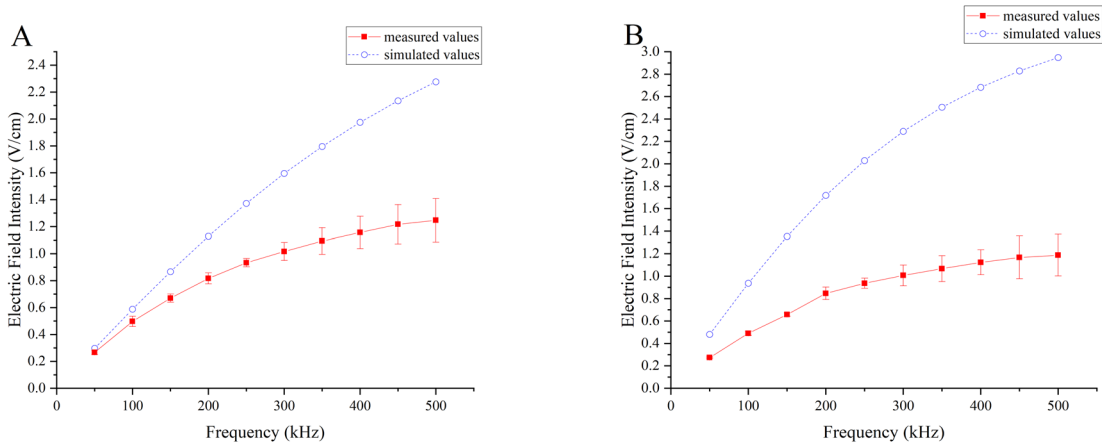

Figure 3. A. Measured and simulated electric field intensity of agar_σ0.78 phantom at different frequencies under the constant voltage source simulation condition. B. Measured and simulated electric field intensity of agar_σ0.48 phantom at different frequencies under the constant voltage source simulation condition.
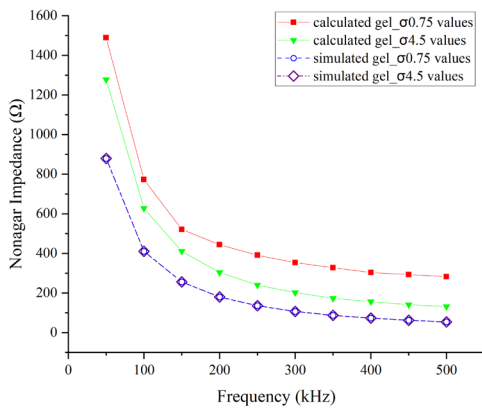

Figure 4. Calculated and simulated non-agar impedance of agar_σ0.78 phantom module with conductive gel of gel_σ0.75 and gel_σ4.5 at different frequencies under constant voltage source condition.

III. RESULTS

D1 and D3 datasets were compared with the two power sources' simulated values at different frequencies respectively. As the simulated result of the constant current source was not affected by the contact medium and transducer's capacitive reactance, the calculated non-agar impedance was compared with the simulated values on voltage source condition to analyze the influence of the contact medium.

A. Simulated and measured values with constant current stimulation

Fig.2A shows the result of the agar_σ0.78 phantom. Current source simulated values have a good agreement with the measured values, their percentage variation is 6.06%. The result of the agar_σ0.48 phantom is shown in Fig.2B. The measured values are similar to the simulated values, their percentage variation is 16.77%.

B. Simulated and measured values with constant voltage stimulation

Fig.3A shows the result of the agar_σ0.78 phantom. Notably, there is an obvious distinction between the simulated and measured values. Fig.3B shows a similar result of the agar_σ0.48 phantom.

C. Effect of contact medium

The calculated non-agar impedance of gel_σ0.75 and gel_σ4.5 on the agar_σ0.78 phantom module is shown in Fig.4. The measured values from the two kinds of conductive gel differed from the simulated values, and there is no difference between the two simulated values.

IV. DISCUSSION AND CONCLUSION

The main purpose of our study is to validate the simulation model of TTFields through actual measurement in phantom. In addition, we further investigated the influence of contact mediums with different conductivities, stimulation conditions, and frequencies on electric fields.

We report a reliable measurement platform for induced EF by TTFields. It is significant for the validation or optimization of the simulation model.

Based on the results obtained under different experimental conditions, we found that the simulated values with the current source were in good accordance with the measured values, especially on the agar_σ0.78 phantom. Our results are consistent with previous studies (Kirson *et al.* and Blatt *et al.)* [2, 6]. Additionally, we further studied the influence of different contact mediums and frequencies on EF intensity. Because the simulation model of the voltage source cannot reflect the contact condition, there was a large difference between measured and simulated values. Furthermore, the conductive gel of gel_σ4.5 produced a smaller non-agar impedance than the gel_σ0.75, which suggested that the contact medium with higher conductivity could produce a lower contact impedance and a higher EF intensity. The magnitude of measured EF increased as the stimulation frequency rose, validating the equal circuit model shown in Fig.1A.

By comparing the simulated and measured values, we conformed that: a) Our measurement platform is a reliable tool to evaluate the EF distribution in the agar phantom. b) Current source simulation for TTFields is a reliable method, even the tissue conductivities and the applied frequency are various. c) For the influence of uncertain contact impedance, voltage source simulation for TTFields is not a good enough method. On the other hand, the voltage source devices are easily available in practical research, but the contact impedance should not be ignored and current monitoring is required when using the voltage source devices for TTFields applications and research.

Our study is not free from limitations. Firstly, the measured values did not match the simulated values on the agar_σ0.48 phantom, the reason might be that the shape of the agar phantom was not symmetrical. Due to repeated measurements, some little holes exist in the agar phantom. Secondly, the agar phantom was prepared in homogeneous for simplicity. It would be desirable to include more complex phantoms or biological tissues. Moreover, the position and number of transducers are significant factors in the EF distribution. The complex combinations of stimulation electrodes should be validated and optimized in further research.

REFERENCES

[1] E. D. Kirson *et al.*, "Disruption of Cancer Cell Replication by Alternating Electric Fields," *Cancer Research,* vol. 64, no. 9, pp. 3288-3295, 2004.

[2] E. D. Kirson *et al.*, "Alternating electric fields arrest cell proliferation in animal tumor models and human brain tumors," (in eng), *Proceedings of the National Academy of Sciences of the United States of America,* vol. 104, no. 24, pp. 10152-10157, 2007.

[3] Y. Porat *et al.*, "Determining the Optimal Inhibitory Frequency for Cancerous Cells Using Tumor Treating Fields (TTFields)," *Journal of visualized experiments : JoVE,* no. 123,

[4] C. Wenger, P. Miranda, A. Mekonnen, R. Salvador, and P. Basser, "Electric fields for the treatment of Glioblastomas: a modelling study," *Neuro-Oncology,* vol. 15, pp. iii235-iii241, 2013.

[5] P. C. Miranda, A. Mekonnen, R. Salvador, and P. J. Basser, "Predicting the electric field distribution in the brain for the treatment of glioblastoma," *Phys Med Biol,* vol. 59, no. 15, pp. 4137-47, 2014.

[6] R. Blatt *et al.*, "In Vivo Safety of Tumor Treating Fields (TTFields) Applied to the Torso," *Frontiers in oncology,* vol. 11, pp. 670809-670809, 2021.

[7] M. Wang, Y. Zheng, H. Guan, J. Zhang, and S. Zhang, "Validation of Numerical Simulation for Transcranial Direct Current Stimulation with Spherical Phantom," in *2020 42nd Annual International Conference of the IEEE Engineering in Medicine & Biology Society (EMBC)*, 2020, pp. 3565-3568.

[8] L. Morales-Quezada, M. M. El-Hagrassy, B. Costa, R. A. McKinley, P. Lv, and F. Fregni, "Transcranial Direct Current Stimulation Optimization – From Physics-Based Computer Simulations to High-Fidelity Head Phantom Fabrication and Measurements," *Methods,* vol. 13, 2019.

[9] C. Gabriel, "Compilation of the dielectric properties of body tissues at RF and microwave frequencies," *Brooks Air Force Technical Report,* vol. AL/OE-TR-1996-0037, 1996.

[10] D. Bennett, "NaCl doping and the conductivity of agar phantoms," *Materials Science and Engineering: C,* vol. 31, no. 2, pp. 494-498, 2011.

[11] R. Plonsey and D. B. Heppner, "Considerations of quasi-stationarity in electrophysiological systems," *The bulletin of mathematical biophysics,* vol. 29, no. 4, pp. 657-664, 1967.

[12] J. D. Johansson, F. Alonso, and K. Wårdell, "Patient-Specific Simulations of Deep Brain Stimulation Electric Field with Aid of In-house Software ELMA," in *2019 41st Annual International Conference of the IEEE Engineering in Medicine and Biology Society (EMBC)*, 2019, pp. 5212-5216: IEEE.

[13] C. Wenger, R. Salvador, P. J. Basser, and P. C. Miranda, "Modeling Tumor Treating fields (TTFields) application within a realistic human head model," in *2015 37th Annual International Conference of the IEEE Engineering in Medicine and Biology Society (EMBC)*, 2015, pp. 2555-2558.

[14] A. R. Korshoej, G. B. Saturnino, L. K. Rasmussen, G. von Oettingen, J. C. H. Sørensen, and A. Thielscher, "Enhancing Predicted Efficacy of Tumor Treating Fields Therapy of Glioblastoma Using Targeted Surgical Craniectomy: A Computer Modeling Study," *PLOS ONE,* vol. 11, no. 10, p. e0164051, 2016.

[15] C. Wenger, R. Salvador, P. J. Basser, and P. C. Miranda, "Improving Tumor Treating Fields Treatment Efficacy in Patients With Glioblastoma Using Personalized Array Layouts," *International Journal of Radiation Oncology*Biology*Physics,* vol. 94, no. 5, pp. 1137-1143, 2016.

[16] Z. Bomzon *et al.*, "Modelling Tumor Treating Fields for the treatment of lung-based tumors," in *2015 37th Annual International Conference of the IEEE Engineering in Medicine and Biology Society (EMBC)*, 2015, pp. 6888-6891.